HHS Public Access

Author manuscript

Am J Med Genet A. Author manuscript; available in PMC 2019 January 01.

Published in final edited form as:

Am J Med Genet A. 2018 January ; 176(1): 92–98. doi:10.1002/ajmg.a.38506.

A homozygous deleterious mutation in *CDK10* is associated with agenesis of corpus callosum, retinopathy and deafness.

Vincent J. Guen[#1], **Simon Edvardson**[#2,3], **Nitay D. Fraenkel**[4], **Aviva Fattal-Valevski**[5], **Chaim Jalas**[6], **Irene Anteby**[7], **Avraham Shaag**[2], **Talia Dor**[3], **David Gillis**[8], **Eitan Kerem**[8], **Jacqueline A. Lees**[1], **Pierre Colas**[9], and **Orly Elpeleg**[2]

[1]David H. Koch Institute for Integrative Cancer Research, Massachusetts Institute of Technology, Cambridge, United States of America.

[2]Monique and Jacques Roboh Department of Genetic Research, Hadassah Medical Center, Hebrew University of Jerusalem, Jerusalem, Israel

[3]Pediatric Neurology Unit, Hadassah Medical Center, Hebrew University of Jerusalem, Jerusalem, Israel.

[4]Department of Respiratory Rehabilitation, Alyn Hospital, Jerusalem, Israel.

[5]Pediatric Neurology Unit, Dana-Dwek Children's Hospital, Tel Aviv Medical Center & Sackler Faculty of Medicine, Tel Aviv University, Tel Aviv, Israel

[6]Bonei Olam, Center for Rare Jewish Genetic Disorders, Brooklyn, NY 11204, USA

[7]Department of Ophthalmology, Hadassah Medical Center, Hebrew University of Jerusalem, Jerusalem, Israel.

[8]Department of Pediatrics, Hadassah Medical Center, Hebrew University of Jerusalem, Jerusalem, Israel.

[9]P2I2 group, Protein Phosphorylation and Human Disease Laboratory, Station Biologique de Roscoff, Centre National de la Recherche Scientifique and Université Pierre et Marie Curie, Roscoff, France.

[#] These authors contributed equally to this work.

Abstract

The primary cilium is a key organelle in numerous physiological and developmental processes. Genetic defects in the formation of this non-motile structure, in its maintenance and function, underlie a wide array of ciliopathies in human, including craniofacial, brain and heart malformations, and retinal and hearing defects.

We used whole exome sequencing to study the molecular basis of disease in an 11-year-old female patient who suffered from growth retardation, global developmental delay with absent speech acquisition, agenesis of corpus callosum and paucity of white matter, sensorineural deafness, retinitis pigmentosa, vertebral anomalies, patent ductus arteriosus, and facial dysmorphism reminiscent of a known ciliopathy, STAR syndrome. A homozygous variant, c.870_871del, was

Corresponding authors: Pierre Colas, colas@sb-roscoff.fr, Orly Elpeleg, Elpeleg@hadassah.org.il.

identified in the *CDK10* gene, predicted to cause a frameshift, p.Trp291Alafs*18, in the cyclin-dependent kinase 10 protein. CDK10 is the binding partner of Cyclin M (CycM) and CDK10/CycM protein kinase regulates ciliogenesis and primary cilium elongation. Notably, CycM gene is mutated in patients with STAR syndrome. Following incubation, the patient cells appeared less elongated and more densely populated than the control cells suggesting that the *CDK10* mutation affects the cytoskeleton. Upon starvation and staining with acetylated-tubulin, γ--tubulin and Arl13b, the patient cells exhibited fewer and shorter cilia than control cells. These findings underscore the importance of CDK10 for the regulation of ciliogenesis. CDK10 defect is associated with a new form of ciliopathy phenotype.

INTRODUCTION

The primary cilium is a solitary microtubule-based structures displayed on the surface of a diverse array of cells in embryonic and adult tissues [1]. Primary ciliogenesis, the dynamic process of assembling the primary cilium, occurs in interphase when a mother centriole is differentiated to form the basal body [2]. The basal body supplies essential components for primary cilium assembly and elongation via the intraflagellar transport machinery [3]. Actin cytoskeleton dynamics plays a key role in ciliogenesis; the assembly of contractile actin filaments represses ciliogenesis. Similarly, nucleating factors which promote actin polymerization repress primary cilium assembly and elongation. In contrast, actin depolymerization activates ciliogenesis by stabilizing the pericentrosomal preciliary compartment, a vesiculo-tubular structure that contributes to ciliogenesis, and by inhibiting transcription factors from the Hippo pathway, which induce the expression of cilium disassembly factors [4–7].

In the last 15 years the primary cilium has emerged as a key organelle in numerous physiological and developmental processes. This non-motile structure acts as a cell signaling center, contributing to normal development through the regulation of major signaling pathways, e.g., Hedgehog and PDGF (reviewed in [1]). Genetic defects in primary cilia formation, maintenance, or function underlie a wide array of ciliopathies in human including craniofacial, brain and heart malformations, and retinal and hearing defects [8–12]. We now report a novel ciliopathy phenotype, associated with *CDK10* mutation, which affects multiple organ systems, including the brain, inner ear, retina and heart.

PATIENT

The subject of this study was an 11 year-old female, the second child to non-consanguineous healthy parents of Ashkenazi-Jewish ancestry. Pregnancy was complicated by intra-uterine growth retardation; agenesis of corpus callosum was noted on ultrasound examination at 32 weeks of gestation. The patient was delivered at 39 weeks of gestation with a birth weight of 1480 gram (−3.7 S.D.) and head circumference of 30.5 cm (−3.0 S.D.). Shortly after birth, heart failure due to a patent ductus arteriosus became apparent, necessitating surgical intervention at 8 months of age. In the aftermath of the surgery, vocal cord paralysis was noted and a tracheostomy was performed. A gastro-jejunostomy was placed at 8 months due to vomiting and failure to thrive. From the age of two years, growth hormone treatment was

initiated with a favorable response. During the second year of life, global developmental delay became apparent but developmental regression was never noted. Physical examination at that time revealed facial dysmorphism which consisted of high forehead, mild bilateral ptosis, upslanting palpebral fissures, telecanthus, broad nasal bridge and long philtrum (figure 1A). Of note, no ano-genital malformations were noted. Further investigations revealed bilateral sensorineural deafness and retinitis pigmentosa with high myopia. Vision in adequate lighting was relatively preserved with glasses and there was no progression of the retinopathy over time. At the time of writing, age 11 years, weight was 31.3 kg and height was 131 cm (15^{th} and 5^{th} percentile, respectively). The patient lacked expressive language but had language understanding that enabled her to follow simple commands. Her cognitive development was consistent with severe intellectual disability with extreme hyperactivity and inattentive behavior. She was ambulant with an unstable broad-based gait; the neurological examination was noted for prominent weakness though creatine kinase level and muscle histology were normal.

Routine laboratory investigations as well as metabolic work-up including plasma amino acids, acylcarnitines, very-long-chain fatty acids, isoelectric focusing of transferrin, lactate and ammonia and urine organic acids, were all within the normal range. Brain MRI at 6 years of age disclosed a rudimentary corpus callosum and paucity of white matter with attendant lateral ventricular widening (Fig.1 B-C). MRI of the spine, performed because of the dysmorphism, disclosed dys-segmentation of C3-C4 and a rudimentary coccyx with adjacent dermal sinus. Of note abdominal ultrasound including kidneys size and shape was normal. Exhaled NO testing was normal as was electron microscopic examination of the nasal cilia.

METHODS

Whole exome analysis

Exonic sequences from the patient DNA sample was enriched with the SureSelect Human All Exon 50 Mb V.5 Kit (Agilent Technologies, Santa Clara, California, USA). Sequences (125-bp paired-end) were generated on a HiSeq2500 (Illumina, San Diego, California, USA). Read alignment and variant calling were performed with DNAnexus (Palo Alto, California, USA) using default parameters with the human genome assembly hg19 (GRCh37) as reference. Parental consent was given for genetic studies. The study was performed with the approval of the ethical committees of Hadassah Medical Center and the Israeli Ministry of Health.

Fibroblasts cell culture and non-sense mediated decay *(NMD) pathway inhibition*

Primary skin fibroblasts were grown until confluence in RPMI 1640 medium with 20 % fetal bovine serum (Sigma-Aldrich) and 1 % penicillin/streptomycin. The cells were treated with 100 μg/mL Cycloheximide (EMD Millipore) for 6 h before RNA extraction to inhibit NMD, or they were serum starved for 24 hours, to induce ciliogenesis, before immunofluorescence experiments.

Immunofluorescence and image analysis

Cells were either fixed in 4% paraformaldehyde for 10 min and permeabilized with 0.3% Triton X100 for 15 min, or fixed and permeabilized with cold methanol for 10 min, and blocked with donkey serum for 1 h before staining with primary antibodies against: acetylated-tubulin (Sigma T7451, 1:1000), γ-tubulin (Thermo Fisher Scientific PA1–28042, 1:1000), Arl13b (Antibodies Inc. 73–287, 1:200). Secondary antibodies were: anti-mouse Alexa Fluor 488 (Life Technologies A11001, 1:1000) or anti-rabbit Alexa Fluor 546 (Life Technologies A11010, 1:1000). Coverslips were mounted on Vectashield with DAPI (Vector Laboratories) and examined using Deltavision Olympus X71 microscope. Images were acquired using a 40X objective and a CoolSNAP HQ camera. Z-stacks were deconvolved (Softworx) and processed with ImageJ.

Quantitative Real Time-PCR

Total RNA was isolated using the PicoPure RNA Isolation Kit (Thermo Fisher Scientific) and cDNAs were generated with random primers and SuperScript III Reverse Transcriptase (Life Technologies). Real-time quantitative PCR reactions were performed with a StepOnePlus Real-Time PCR system (Life Technologies) using the Fast SYBR Green PCR Master Mix (Life Technologies) and the following primers: CDK10 forward - GAAGGATGGCATCCCCATCAGC, CDK10 reverse - CCAGGTCCTGCTCACAGTAACC, PTBP1 forward - GAGTCACACCCCAAAGCCTCTT, PTBP1 reverse - CACGTTCTGGTGCTTCGAGAGC, GAPDH forward - TGCACCACCAACTGCTTAGC, GAPDH reverse – GGCATGGACTGTGGTCATGAG (used for normalization).

RESULTS

Whole exome analysis yielded 44.2 million mapped reads with a mean coverage of X76. Following alignment and variant calling, we removed variants which were called less than X8, were off-target, synonymous, had minor allele frequency (MAF)>0.5% or were homozygous at ExAC (Exome Aggregation Consortium, Cambridge, MA, (URL: http://exac.broadinstitute.org)) or MAF>2% at the Hadassah in-house database (2200 exome analyses). 204 variants remained, including 3 homozygous variants, p. R-500-Q in *SCUBE1*, p.L-618-M in *TCF25*, and c.870_871del in *CDK10*. We focused on the later, Hg19 Chr16: 89761416–7 delAT (rs766960979), NM_052988.4:c.870_871del, p.Trp291Alafs*18 in the cyclin-dependent kinase 10 (*CDK10*) gene because of its deleterious nature. Importantly, CDK10 is the binding partner of CycM, which is encoded by *FAM58A* [13]. *FAM58A* is mutated in patients with STAR syndrome who present with facial dysmorphism reminiscent of that of our patient (figure 1D).

The *CDK10* c.870_871del variant is carried by 36 of the ~141,000 healthy individuals whose exome and genome analyses are deposited at gnomAD website [14]; nearly all of the carriers for this variant are of Ashkenazi-Jewish descent, accounting for a carrier rate of 1/290 in this community. Importantly, no homozygous LOF variants in this gene are present in the entire gnomAD cohort [14]. Sanger sequencing confirmed segregation of the c.870_871del with the disease in the family (figure 2A). To examine the consequences of the

variant at the RNA level, we studied *CDK10* mRNA abundance and noted slightly increased level in the patient compared to the control cells (figure 2B). Importantly, the *CDK10* mRNA level remained unchanged when the patient cells were incubated with cycloheximide [15], in contrast to the *PTBP1* mRNAs, which serves as a control because it is known to be subjected to non-sense mediated decay (NMD). This result indicates that the *CDK10* mutant RNA is not degraded by the NMD pathway (figure 2C).

Our recent work showing that the CDK10/ Cyclin M (CycM) protein kinase regulates ciliogenesis and primary cilium elongation [16] prompted us to examine primary cilia on the patient fibroblasts. 24h after plating, at low confluence, a morphological difference could be observed between the patient and control fibroblasts with the patient cells appearing less elongated than the control cells, suggesting that the *CDK10* mutation affects the cytoskeleton (Figure 3A). When the cells reached confluence, this morphological difference appeared even more striking and the patient cells were more densely populated than the control cells (not shown). We then starved the cells for 24h to induce ciliogenesis, and observed primary cilia and centrosomes via acetylated-tubulin and γ-tubulin staining, respectively. Whereas control cells exhibited normal primary cilia protruding from centrosomes, the patient cells exhibited absent or shorter cilia and weaker γ-tubulin staining (Figure 3B). To confirm these observations, we stained the cells for Arl13b, another marker of primary cilia, observing again, fewer and shorter cilia on patient cells as compared to the control cells (Figure 3C, D, E).

DISCUSSION

The patient report herein suffered from growth retardation, global developmental delay with absent speech acquisition, agenesis of corpus callosum and paucity of white matter, sensorineural deafness, retinitis pigmentosa, vertebral anomalies, patent ductus arteriosus, and facial dysmorphism. The facial dysmorphism consisted of high forehead, upslanting palpebral fissures, telecanthus, broad nasal bridge, and long philtrum. As mentioned above, CDK10, the identified mutated gene, is the binding partner of CycM [13], the protein mutated in patients with STAR syndrome. These patients present with facial dysmorphism which bears similarity to that of our patient (figure 1B), syndactyly, ano-urogenital malformations, short stature and variable heart and eye abnormalities; the syndrome is transmitted in an X-linked dominant manner[17,18],.

CDK10 and CycM form a heterodimeric protein kinase; silencing each one of them phenocopies silencing the other [13]. We have previously shown that CDK10/CycM is a repressor of ciliogenesis via its role in the promotion of actin network formation through phosphorylation of PKN2 and promotion of RhoA signaling. CDK10/CycM is localized to the base of primary cilia, concentrated at the mother centriole [16]. In quiescent immortalized retinal pigmented epithelial (RPE) cells, knocking down CDK10 or CycM resulted in significant increase in the number of ciliated cells, abnormally long cilia and promotion of the maintenance of primary cilia upon cell cycle re-entry [16]. The actin network was disrupted and actin stress fibers were lost in the absence of CDK10 or CycM. Extensive screen for CDK10/CycM phosphorylation substrates identified several proteins, all known regulators of actin dynamics. Knocking down PKN2, (which is one of these

regulators), or simply abolishing PKN2 aminoacids that are phosphorylated by CDK10/CycM, mimicked CDK10 or CycM deficiency, with a decrease of actin stress fibers, and an increase in both ciliogenesis and in cilia length. Concomitantly, PKN2 deficiency resulted in a destabilization of the GTPase RhoA, a protein that can repress ciliogenesis. These findings and the observation that kidney sections from a STAR patient display dilated renal tubules and elongated cilia, led us to propose that STAR syndrome, which is associated with mutations in the *CycM* gene, is a ciliopathy [16].

The present report underscores the importance of CDK10 for normal regulation of ciliogenesis; the homozygous c.870_871del mutation in the *CDK10* gene is associated with severe developmental defects and abnormal primary cilia. However, in contrast to the increased ciliogenesis with abnormally long cilia observed in STAR patients with *CycM* loss-of-function mutations or in the experimental CDK10/CycM knockdown, the homozygous *CDK10* c.870_871del mutation results in shorter, less abundant cilia. We therefore examined *CDK10* mRNA abundance in the patient and control cells and noted that the mutant *CDK10* mRNA is not degraded by the NMD pathway; this result suggests that instead of the WT 360 amino acids long CDK10 protein, a shorter, 307 residues long isoform is produced, containing missense 17 amino acids at its C-terminus. If expressed, this mutant would be devoid of the C-terminal bipartite nuclear localization sequence, while potentially retaining its ability to interact with CycM, two features that may phenocopy the naturally-occurring shorter CDK10 isoforms produced from the highly complex alternative splicing events concerning the *CDK10* gene [19]. As observed in a number of proteins playing multiple, complex regulatory roles, the different WT CDK10 isoforms are suspected to exert distinct, perhaps partly opposing functions [20]. We therefore speculate that the shorter mutant CDK10 protein loses some of the functions exerted by the WT CDK10, at the advantage of other extra-nuclear functions such as ciliogenesis inhibition. Since heterozygous individuals are asymptomatic, it is conceivable that this mutated polypeptide is counterbalanced by WT isoforms and would only produce effects in a homozygous context.

Thus, CDK10 defect is associated with a new form of ciliopathy phenotype, bearing clinical similarity to CycM defect only in the facial appearance of the patients, and sharing the retinal involvement, the hearing loss and the short stature with many patients with ciliopathies including Senior–Løken syndrome, Bardet-Biedl syndrome and Alström syndrome, and the corpus callosum agenesis with patients suffering from KIF7 and OFD1 ciliopathies [21,22].

Supplementary Material

Refer to Web version on PubMed Central for supplementary material.

ACKNOWLEDGEMENT:

This work was supported in part by the Trudy Mandel Louis Charitable Trust to OE

REFERENCES

1. Goetz SC, Anderson KV. (2010) The primary cilium: a signalling centre during vertebrate development. Nat Rev Genet. 11:331–344 [PubMed: 20395968]
2. Ishikawa H, Marshall WF. (2011) Ciliogenesis: building the cell's antenna. Nat Rev Mol Cell Biol 12:222–234 [PubMed: 21427764]
3. Taschner M, Lorentzen E. (2016) The Intraflagellar Transport Machinery. Cold Spring Harb Perspect Biol. 8:a028092 [PubMed: 27352625]
4. Kim J, Lee JE, Heynen-Genel S, Suyama E, Ono K, Lee K, Ideker T, Aza-Blanc P, Gleeson JG . (2010) Functional genomic screen for modulators of ciliogenesis and cilium length. Nature 464:1048–1051 [PubMed: 20393563]
5. Cao J, Shen Y, Zhu L, Xu Y, Zhou Y, Wu Z, Li Y, Yan X, Zhu X (2012) miR-129–3p controls cilia assembly by regulating CP110 and actin dynamics. Nat Cell Biol 14:697–706 [PubMed: 22684256]
6. Bershteyn M, Atwood SX, Woo WM, Li M, Oro AE (2010) MIM and cortactin antagonism regulates ciliogenesis and hedgehog signaling. Dev Cell 19:270–283 [PubMed: 20708589]
7. Kim J, Jo H, Hong H, Kim MH, Kim JM, Lee JK, Heo WD, Kim J. (2015) Actin remodelling factors control ciliogenesis by regulating YAP/TAZ activity and vesicle trafficking. Nat commun 6:6781 [PubMed: 25849865]
8. Tian H, Feng J, Li J, Ho TV, Yuan Y, Liu Y, Brindopke F, Figueiredo JC, Magee W, 3rd, Sanchez-Lara PA, Chai Y. (2017) Intraflagellar transport 88 (IFT88) is crucial for craniofacial development in mice and is a candidate gene for human cleft lip and palate. Hum Mol Genet. doi: 10.1093/hmg/ddx002
9. Guemez-Gamboa A, Coufal NG, Gleeson JG. (2014) Primary cilia in the developing and mature brain. Neuron 82:511–521 [PubMed: 24811376]
10. Willaredt MA, Gorgas K, Gardner HA, Tucker KL. (2012) Multiple essential roles for primary cilia in heart development. Cilia 1:23 [PubMed: 23351706]
11. Yildiz O, Khanna H. (2012) Ciliary signaling cascades in photoreceptors. Vision Res 75:112–116 [PubMed: 22921640]
12. May-Simera H, Kelley MW. (2012) Planar cell polarity in the inner ear. Curr Top Dev Biol 101:111–140. [PubMed: 23140627]
13. Guen VJ, Gamble C, Flajolet M, Unger S, Thollet A, Ferandin Y, Superti-Furga A, Cohen PA, Meijer L, Colas P. (2013) deficient in STAR syndrome. Proc Natl Acad Sci U S A 110:19525–19530. [PubMed: 24218572]
14. Lek M, Karczewski KJ, Minikel EV, et al. (2016) Analysis of protein-coding genetic variation in 60,706 humans. Nature 536:285–291 [PubMed: 27535533]
15. Carter MS1, Doskow J, Morris P, Li S, Nhim RP, Sandstedt S, Wilkinson MF (1995) A regulatory mechanism that detects premature nonsense codons in T-cell receptor transcripts in vivo is reversed by protein synthesis inhibitors in vitro. J Biol Chem. 270:28995–29003. [PubMed: 7499432]
16. Guen VJ, Gamble C, Perez DE, Bourassa S, Zappel H, Gärtner J, Lees JA, Colas P. (2016) STAR syndrome-associated CDK10/Cyclin M regulates actin network architecture and ciliogenesis. Cell Cycle 15:678–688. [PubMed: 27104747]
17. Unger S, Böhm D, Kaiser FJ, Kaulfuss S, Borozdin W, Buiting K, Burfeind P, Böhm J, Barrionuevo F, Craig A, Borowski K, Keppler-Noreuil K, Schmitt-Mechelke T, Steiner B, Bartholdi D, Lemke J, Mortier G, Sandford R, Zabel B, Superti-Furga A, Kohlhase J. (2008) Mutations in the cyclin family member FAM58A cause an X-linked dominant disorder characterized by syndactyly, telecanthus and anogenital and renal malformations. Nat Genet 40:287–289 [PubMed: 18297069]
18. Zarate YA, Farrell JM, Alfaro MP, Elhassan NO (2015) STAR syndrome is part of the differential diagnosis of females with anorectal malformations. Am J Med Genet A. 167A:1940–1943. [PubMed: 25845904]
19. Sergère JC, Thuret JY, Le Roux G, Carosella ED, Leteurtre F. (2000) Human CDK10 gene isoforms. Biochem Biophys Res Commun. 276:271–277. [PubMed: 11006117]

20. Guen VJ, Gamble C, Lees JA, Colas P (2017). The awakening of the CDK10/Cyclin M protein kinase. Oncotarget. doi: 10.18632/oncotarget.15024

21. Barakeh D, Faqeih E, Anazi S, S Al-Dosari M, Softah A, Albadr F, Hassan H, Alazami AM, Alkuraya FS. (2015) The many faces of KIF7. Hum Genome Var 2:15006 [PubMed: 27081521]

22. Del Giudice E, Macca M, Imperati F, D'Amico A, Parent P, Pasquier L, Layet V, Lyonnet S, Stamboul-Darmency V, Thauvin-Robinet C, Franco B; Oral-Facial-Digital Type I (OFD1) Collaborative Group (2014) CNS involvement in OFD1 syndrome: a clinical, molecular, and neuroimaging study. Orphanet J Rare Dis 9:74 [PubMed: 24884629]

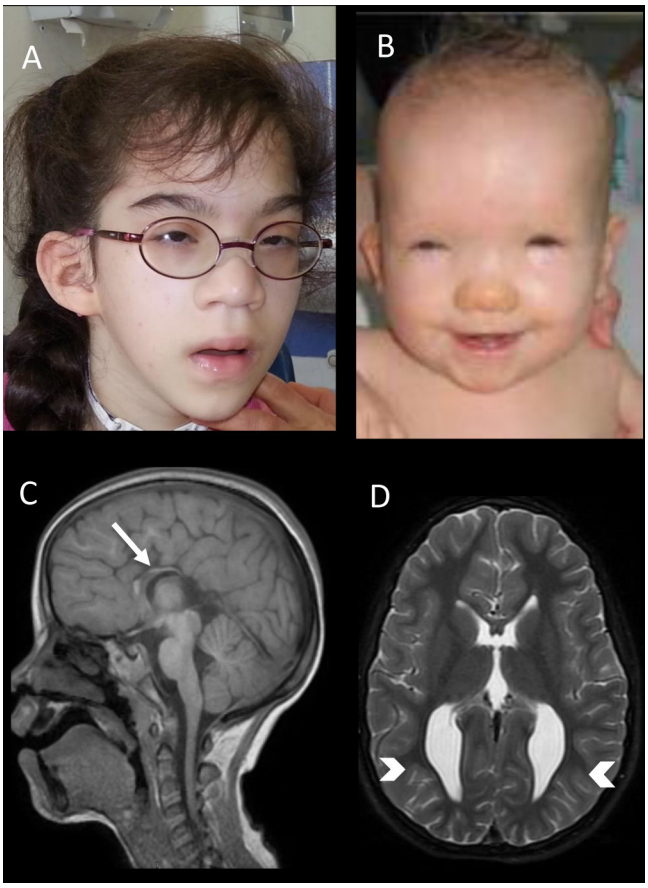

Figure 1: Clinical and radiological features.

Patient face (A) note high forehead, bilateral ptosis, upslanting palpebral fissures, telecanthus, broad nasal bridge, and long philtrum. Patient brain MRI at 6 years of age (midsagittal T1-weighted (B) and Axial T2-weighted (C) images) showing rudimentary corpus callosum (arrow) and paucity of white matter around posterior horns of lateral ventricles (arrowheads). Face of a patient with STAR syndrome is shown in order to demonstrate the striking resemblance (D) (reprinted by permission from Macmillan Publishers Ltd [17]).

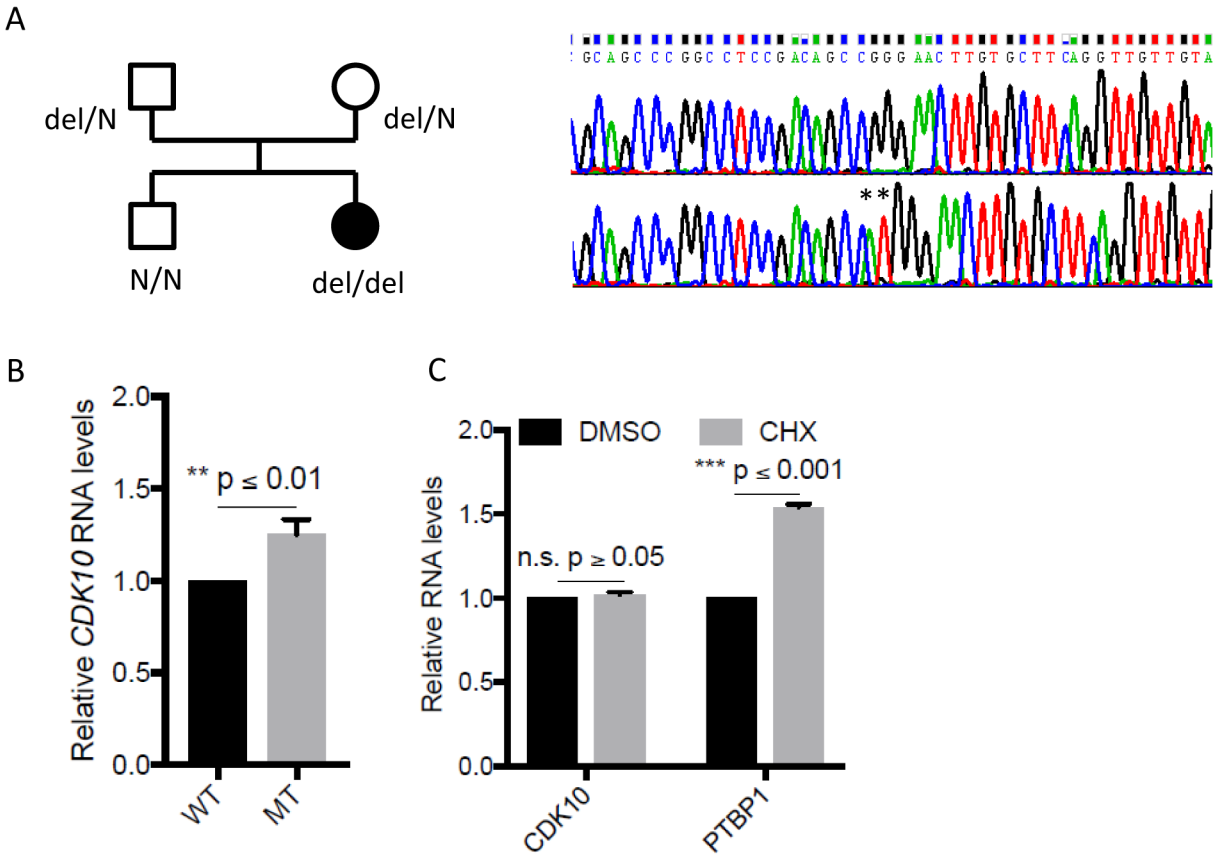

Figure 2: CDK10 DNA and mRNA in control and patient cells.

(A) Genotype in the family (left panel) and DNA sequencing around the c.870_871del variant in *CDK10* in the patient (right upper panel) and the healthy brother (right lower panel); the deleted bases are marked by asterisk. (B) Real-time quantitative PCR analysis of CDK10 RNA levels in control (WT) and patient (MT) cells. (C) Real-time quantitative PCR analysis of CDK10 or PTBP1 RNA levels in patient cells treated or not with cycloheximide (CHX).

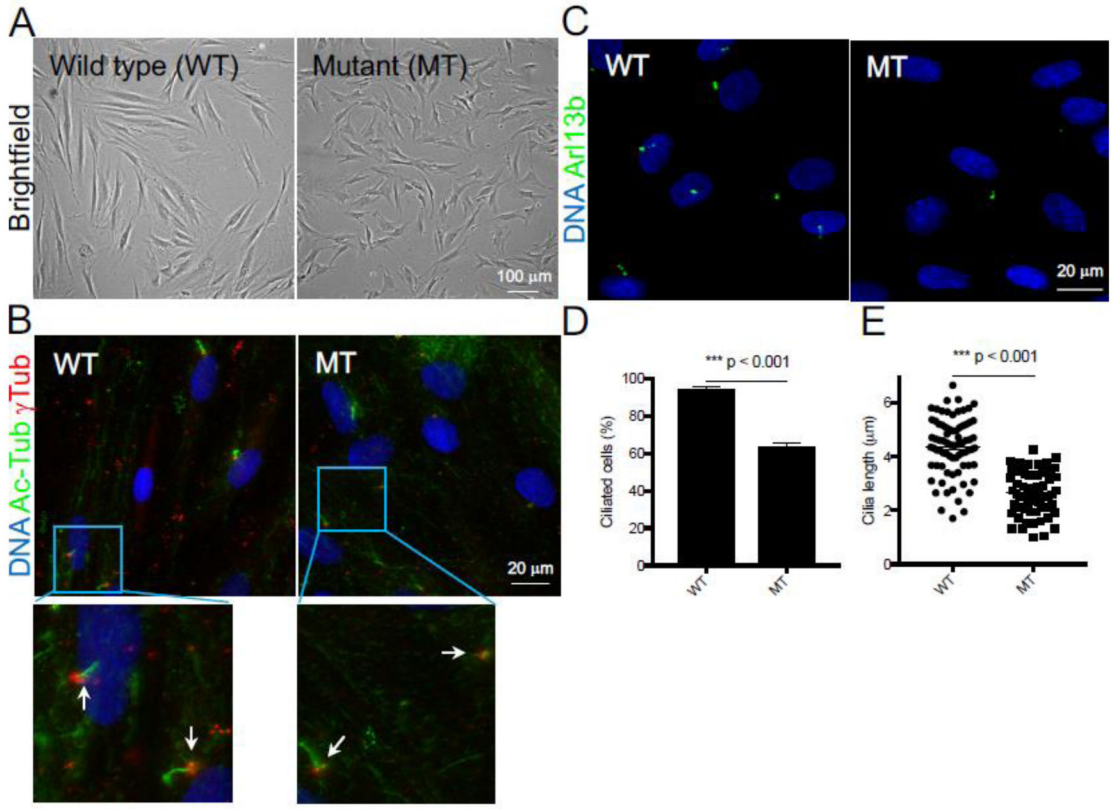

Figure 3: Primary cilia defects in patient's fibroblasts.

(A) Brightfield observation of fibroblasts obtained from a healthy, control individual (WT) and from the patient (MT). (B) Representative immunofluorescence images of primary cilia (acetylated-tubulin staining, shown in green), centrosomes (γ-tubulin staining, shown in red), and DNA (DAPI staining, shown in blue). (C) Representative immunofluorescence images of primary cilia (Arl13b staining, shown in green) and DNA (DAPI staining, shown in blue). The percent of cells with primary cilia (D) and cilia length (E) was determined from 3 independent Arl13b staining experiments, counting each time at least 100 cells.